Metallic Aluminum Nanorods: Synthesis via Vapor-Deposition and Applications in Al/air Batteries

Chunsheng Li, Weiqiang Ji, Jun Chen,* and Zhanliang Tao

Institute of New Energy Material Chemistry, Nankai University, Tianjin 300071, P. R. China

Received July 17, 2007
Revised Manuscript Received September 22, 2007

In recent years, electrochemical storage and conversion of energy in batteries has become increasingly significant for various applications.[1–5] Compared with other battery systems, the aluminum/air battery, one of the most important metal/air batteries, is especially suitable for being a power device because of its advantages: (1) a high theoretical energy density (8.1 kW h kg^{-1}-A1), (2) a high theoretical voltage (2.74 V), (3) low cost, and (4) nontoxicity for the environment.[6,7] For the Al/air battery, the anode is made of a reactive metallic Al, whereas the cathode is an air electrode provided by an inexhaustible reactant from oxygen in the air.[8–11] In the commercial Al/air batteries, the Al electrodes were generally prepared from highly pure Al sheets or powders with the shortages of low current density and low utilization efficiency of the active materials. Recently, Al nanoparticles and nanowires have been prepared by various methods such as electromigration, electron-beam direct-writing lithography, and template processing.[12–14] However, to the best of our knowledge, the rational control of Al nanorods and their further battery application have been rarely seen. Herein, we report on the fabrication of Al nanorods by a facile vapor-deposition method and further demonstrate their promising electrochemical performance in Al/air batteries.

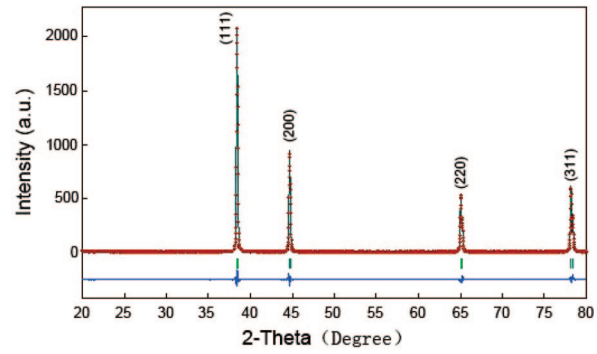

Figure 1. X-ray diffraction profile of the as-prepared Al nanorods: observed (red points), calculated (blue line), and difference (bottom blue line). Vertical bars below the patterns show the positions of all possible reflection peaks. The *hkl* labels are placed according to the reflection position.

The experimental device for the preparation of Al nanorods was similar to that described previously to prepare metallic magnesium and zinc nano/meso/microscale structures.[8,15] In brief, commercial Al powders with a purity of 99.99% (Tianjin Jinke Fine Chemical Institute) loaded in tungsten boats were positioned at the middle of a horizontal ceramic tube that was mounted in the center of a conventional tube furnace. The center part of the furnace was heated at a rate of 30 °C/min to 1000 °C, and then kept at this temperature for 10 h. A constant flow of high-purity Ar (99.999%, BOC Gases from Tianjin Co. Ltd.) at a flow rate of 1000 cm^3/min was maintained during both the temperature increasing and decreasing steps. After being cooled to room temperature naturally, dark gray wool-like products were obtained on the inner wall of the ceramic tube and the surface of the substrate at the cooling temperature region of 240–270 °C. All the samples obtained from different temperature regions were collected with the protection of Ar gas flows and then stored in a glovebox (Mikrouna China Universal 2240/750) to prevent oxidation/corrosion of Al.

The structures of the as-prepared products were characterized by powder X-ray diffraction (XRD) using a Rigaku D/max-2500 X-ray generator with Cu Kα radiation. The size and morphology of the products were examined by a JEOL JSM-6700F field emission scanning electron microscopy (SEM). The transmission electron microscopy (TEM) and high-resolution TEM (HRTEM) images were taken on FEI Tecnai 20 transmission electron microscope at an accelerating voltage of 200 kV.

Figure 1 shows the representative rietveld refinement of XRD patterns of the as-deposited Al nanorods. It can be seen that the refined patterns fit the observed data points very well. No peak from another phase has been detected in the samples, revealing that the as-synthesized products are of high Al purity. The cell parameters of the Al can be determined to be $a = 4.04498$ Å, corresponding well with the standard values (space group *Fm*–3*m*, JCPDS-ICDD Card 04-0787).

* Corresponding author. E-mail: chenabc@nankai.edu.cn. Fax: (86) 22-2350-9118.

(1) Tarascon, J. M.; Armand, M. *Nature* **2001**, *414*, 359.
(2) Sorensen, E. M.; Izumi, H. K.; Vaughey, J. T.; Stern, C. L.; Poeppelmeier, K. R. *J. Am. Chem. Soc.* **2005**, *127*, 6347.
(3) Winter, M.; Brodd, R. J. *Chem. Rev.* **2004**, *104*, 4245.
(4) Long, J. W.; Dunn, B.; Rolison, D. R.; White, H. S. *Chem. Rev.* **2004**, *104*, 4463.
(5) Wang, Y.; Cao, G. Z. *Chem. Mater.* **2006**, *18*, 2787.
(6) (a) Zhang, X.; Yang, S. H.; Knickle, H. *J. Power Sources* **2004**, *128*, 331. (b) Yang, S. H.; Knickle, H. *J. Power Sources* **2002**, *112*, 162. (c) Li, Q. F.; Bjerrum, N. J. *J. Power Sources* **2002**, *110*, 1.
(7) (a) Licht, S.; Levitin, G.; Tel-Vered, R.; Yarnitzky, C. *Electrochem. Commun.* **2000**, *2*, 329. (b) Han, B.; Liang, G. C. *Rare Met.* **2006**, *25*, 360.
(8) Li, W. Y.; Li, C. S.; Zhou, C. Y.; Ma, H.; Chen, J. *Angew. Chem. Int. Ed.* **2006**, *45*, 6009.
(9) Ngala, J. K.; Alia, S.; Dobley, A.; Crisostomo, V. M. B.; Suib, S. L. *Chem. Mater.* **2007**, *19*, 229.
(10) Crisostomo, V. M. B.; Ngala, J. K.; Alia, S.; Dobley, A.; Morein, C.; Chen, C. H.; Shen, X. F.; Suib, S. L. *Chem. Mater.* **2007**, *19*, 1832.
(11) Chan, K. Y.; Savinell, R. F. *J. Electrochem. Soc.* **1991**, *138*, 1976.
(12) (a) Saka, M.; Nakanishi, R. *Mater. Lett.* **2006**, *60*, 2129. (b) Saka, M.; Ueda, R. *J. Mater. Res.* **2005**, *20*, 2712.
(13) (a) Wang, J. J.; Liu, F.; Deng, X. G.; Liu, X. M.; Chen, L.; Sciortino, P.; Varghese, R. *J. Vac. Sci. Technol. B* **2005**, *23*, 3164. (b) Chen, Y. J.; Hsu, J. H.; Lin, H. N. *Nanotechnology* **2005**, *16*, 1112.
(14) Pang, Y. T.; Meng, G. W.; Zhang, L. D.; Shan, W. J.; Zhang, C.; Gao, X. Y.; Zhao, A. W. *Solid State Sci.* **2003**, *5*, 1063.
(15) Ma, H.; Li, C. S.; Su, Y.; Chen, J. *J. Mater. Chem.* **2007**, *17*, 684.

10.1021/cm7018795 CCC: $37.00
Published on Web 10/24/2007

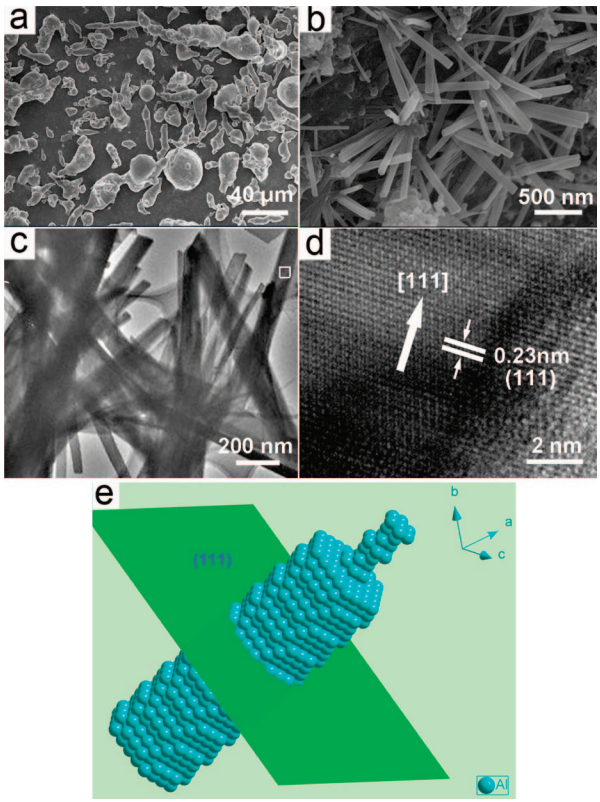

Figure 2. Typical scanning electron microscopy (SEM) images of the Al products: (a) commercial Al powders, (b) as-deposited Al nanorods; (c) representative transmission electron microscopy (TEM) image of Al nanorods; and (d) high-resolution transmission electron microscopy (HRTEM) image of the white square marked in image c. (e) Schematic crystal structure of Al nanorods.

Figure 2 shows the morphologies and microstructures of the commercial Al powders and the as-deposited Al nanorods. The SEM image in Figure 2a demonstrates the particle size of 5–30 μm for the commercial Al powders. Figure 2b shows the SEM image of Al nanorods obtained at the conditions of an evaporation temperature of 1000 °C, a deposition temperature of 250 °C, and a deposition time of 10 h with an argon flow rate of 1000 cm^3/min. It can be seen that a large number of Al nanorods with smooth surfaces are tightly fixed on the surface of the stainless-steel substrate. The diameter of the nanorods is approximately 30–90 nm. Further insight into the microstructure of the Al nanorods are investigated by TEM and HRTEM. The TEM image in Figure 2c reveals that the lengths of the nanorods are in the range of 1–2 μm. Figure 2d shows the HRTEM image of part of an Al nanorod. Clear fringes with an interplanar spacing of 0.23 nm can be observed, which is in accordance with the *d*-spacings between the (111) crystal planes, indicating that the Al nanorod grows along the [111] direction (marked by the white arrow in Figure 2d). Figure 2e shows the crystal structure of the Al nanorods, in which the stacking of aluminum atoms in a typical face-centered cubic (fcc) type. As marked in the picture, the green plan stands for the (111) lattice plan, which is perpendicular to the preferred orientation vector [111]. Interestingly, the spacing between layers (*d*-spacing of two (111) planes) in Figure 2e is consistent with the distance of the neighboring fringes shown in Figure 2d. According to the results presented above, the formation of the Al nanorods, which were prepared through the vapor-transport approach, follows a vapor-solid (VS) growth mechanism.[16] Because no additional metals were employed as the catalyst and no droplets were observed at the tips of the nanorods in both SEM and TEM images (Figures 2b and 2c), we could rule out the vapor–liquid–solid (VLS) mechanism.[17–19] In addition, the mixture of micro- and nanoscale products can be synthesized by changing experimental parameters, including the evaporation temperature, deposition time, and flow rate.

Aluminum electrodes were prepared in a glovebox by inserting the mixture of active materials (vapor-deposited Al nanorodes or commercial high-purity Al powders), Vulcan XC-72 carbon (Cabot), and poly(tetrafluoroethylene) (PTFE) into glass-tube electrodes. The mold of glass-tube electrodes was similar to those applied in our previous works on Mg/air and Zn/MnO_2 batteries.[8,15] The electrode was made of a glass tube (2.1 mm in inner diameter, 2.5 mm in outer diameter, and 15.0 mm in length), ethoxyline resin, and copper collector. The electrochemical measurements of linear sweep voltammograms and impedance spectra of aluminum electrodes were carried out with a Parstat 2273 potentiostat/galvanostat analyzer (AMTECT Co.) using three-electrode cells that contain Al glass-tube electrode as described above, a platinum sheet (1 cm^2) as counter electrode, and Ag/AgCl–KCl (saturated) as reference electrode. The nonaqueous electrolyte used in the system was 4 M KOH/ethanol solution, which can provide extremely low corrosion current, high current density, and high negative potential for the electrode.[20]

The laboratory-made Al/air batteries comprised the Al anode, a spacer, and an air cathode. The Al mixture was carefully pressed on the surface of a copper collector to form Al anode for investigating the discharge performance. The air electrode comprised a gas diffusion layer and an active layer, which separates the air and the 4 M KOH/ethanol electrolyte. In the active and hydrophilic layer, $La_{0.6}Ca_{0.4}CoO_3$ perovskite catalyst was used, which had been established to be the best candidate as electrocatalyst in alkaline electrolytes for air electrodes.[21] The discharging performances were examined by an LAND CT2001A charge–discharge device at the temperature of 25 °C. Two kinds of mixtures for Al anode were investigated. Mixture I consists of 65 wt% active materials, 25 wt% carbon, and 10 wt% PTFE, whereas mixture II is made of 80 wt% active materials, 10 wt% carbon, and 10 wt% PTFE.

Figure 3 shows the linear sweep voltammograms of Al electrodes made from the as-deposited Al nanorods and commercial Al powders with two kinds of mixtures in 4 M KOH/ethanol solution. The composition of these four Al electrodes

(16) Ma, R. Z.; Bando, Y. *Chem. Mater.* **2002**, *14*, 4403.
(17) Rao, C. N. R.; Deepak, F. L.; Gundiah, G.; Govindaraj, A. *Prog. Solid State Chem.* **2003**, *31*, 5.
(18) Wang, Y. W.; Meng, G. W.; Zhang, L. D.; Liang, C. H.; Zhang, J. *Chem. Mater.* **2002**, *14*, 1773.
(19) Mathur, S.; Shen, H.; Sivakov, V.; Werner, U. *Chem. Mater.* **2004**, *16*, 2449.
(20) Shao, H. B.; Wang, J. M.; Wang, X. Y.; Zhang, J. Q.; Cao, C. N. *Electrochem. Commun.* **2004**, *6*, 6.
(21) Zhang, G. Y.; Chen, J. *J. Electrochem. Soc.* **2005**, *152*, A2069.

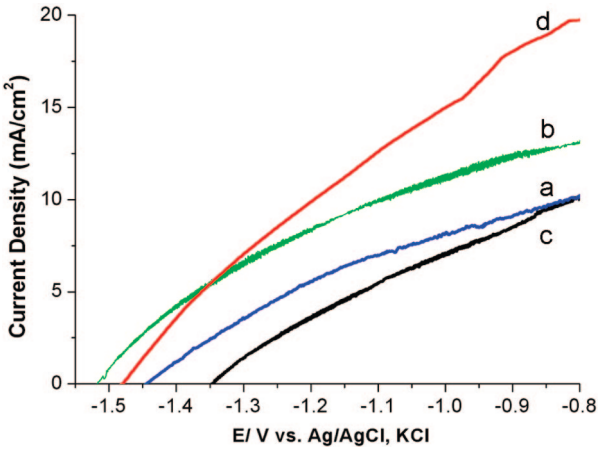

Figure 3. Linear sweep voltammograms of Al electrodes made from different morphologies of Al in two kinds of mixtures: (a) commercial Al powder electrode in mixture I; (b) commercial Al powder electrode in mixture II; (c) Al nanorod electrode in mixture II; (d) Al nanorod electrode in mixture I with a nonaqueous electrolyte solution of 4 M KOH/ethanol. Scan rate: 20 mV s^{-1}.

are listed in Table S1 in the Supporting Information . The potential of the curves is scanned from −1.60 to −0.80 V versus Ag/AgCl saturated with KCl at a scan rate of 20 mV s^{-1}. As shown in Figure 3, all of the anodic dissolution current densities of the Al electrodes greatly increase as the potential sweeps from −1.6 to −0.8 V. The anodic dissolution current densities of commercial Al powders increase with enhancing the composition of mixtures from 65 wt% (Figure 3a) to 80 wt% (Figure 3b). In addition, the starting potential of the Al anodic dissolution in mixture II (−1.52 V) is much higher than that of mixture I (−1.45 V). In general, a more negative anodic dissolution potential is favorable for improving the open circuit voltage and discharge capacity for the Al/air battery. When the electrodes made from the as-deposited Al nanorods were prepared according to the composition of mixture II (Figure 3c), both the starting potential and the current density of anodic dissolution are lower than those of the curves in plots a and b in Figure 3. This demonstrates that higher composition of Al nanomaterials in mixture II probably reduces the contact behaviors with the other electrode materials such as carbon and PTFE, leading to poor electrochemical performances of the electrodes. When the composition of the electrodes is reduced to 65 wt%, the anodic dissolution current densities of the electrodes made from the Al nanorods (Figure 3d) are much higher than that of the electrodes made from the commercial Al powders (plots a and b in Figure 3). The sequence of current densities from highest to lowest is d > b > a > c. These results indicate that the electrochemical activity of the as-deposited Al nanostructures is higher than that of commercial Al powders, even at a low composition of the mixture. In addition, electrochemical impedance spectroscopy (EIS) of Al nanorods and commercial Al powders is also investigated (see Figure S1 in the Supporting Information).

Figure 4 shows typical discharge curves for Al/air batteries made from commercial Al powders and as-prepared Al nanorods. The weights of active material for commercial and as-deposited Al in the battery are 21.9 and 19.9 mg, respectively. The inset in Figure 4 is the laboratory-made Al/air button cells (diameter, 20mm). The open-circuit

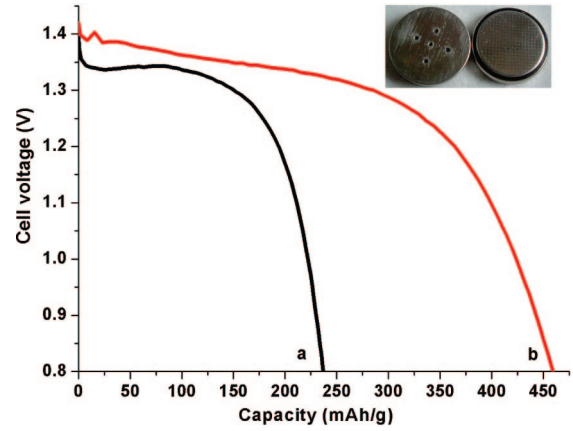

Figure 4. Typical discharge curves of the Al/air batteries made from (a) commercial Al powders in mixture II, (b) as-prepared Al nanorods in mixture I at a constant current density of 0.7 mA/cm^2. The inset is the laboratory-made Al/air batteries.

voltage of the battery made from the as-deposited Al nanorods is approximately 1.42 V, showing voltage similar to that of the battery made from commercial Al powders (approximately 1.40 V). It is noted that the battery made from Al nanorods presents a higher average operating voltage (approximately 1.35 V) and a much higher specific capacity (458 mA h g^{-1}, Figure 4b) than that made from commercial Al powders (236 mA h g^{-1}, Figure 4a). However, the capacity of commercial Al/air battry in Altek Fuel Group Inc. (model APS 100–12) is 324 mA h g^{-1} (electrical capacity, 120 A h; Al anode weight, 0.37 kg).[22] According to the results presented above, Al nanorods with higher specific surface areas exhibit superior electrochemical properties and are promising candidates for Al/air batteries. However, the practical open-circuit voltage and energy density are still lower than the theoretical limit (theoretical voltage of 2.74 V and theoretical energy density of (8.1 kW h kg^{-1}-A1). The reason is because of the corrosion of aluminum and the formation of the oxide film.[6c,20]

In summary, Al nanorods were successfully prepared via a vapor-deposition method through the evaporation of Al powders at a suitable experimental condition. The electrode made from the as-deposited Al nanorods with the composition of 65 wt% Al, 25 wt% carbon, and 10 wt% PTFE exhibits superior electrochemical properties to that made from commercial Al powder. Furthermore, the laboratory-made Al/air battery with the as-prepared Al nanorods displays high discharge specific capacity and average operating voltage, which is important for developing long-life battery systems.

Acknowledgment. This work was supported by National NSFC (20325102) and 973 Project (2005CB623607).

Supporting Information Available: The composition of four different Al electrodes and electrochemical impedance spectroscopy (EIS) of commercial Al powders and Al nanorods (PDF). This material is available free of charge via the Internet at http://pubs.acs.org.

CM7018795

(22) http://altekfuel.com/userfiles/File/SDS_APS100_12-24_V-04.pdf